

# Nuclear astrophysics experiments: Reactions and elastic scattering

J.-S. Graulich, R. Coszach<sup>a</sup>, and P. Leleux

Université catholique de Louvain, B-1348 Louvain-la-Neuve, Belgium

Received: 1 May 2001 / Revised version: 12 June 2001

**Abstract.** Experimental methods in nuclear astrophysics experiments with radioactive beams are described, and evaluated. The importance of performing the (p, p) elastic scattering in parallel to a (p,  $\alpha$ ) or a (p,  $\gamma$ ) reaction is emphasized.

**PACS.** 26.50.+x Nuclear physics aspects of novae, supernovae and other explosive environments – 27.20.+n  $6 \leq A \leq 19$

## 1 Introduction

The understanding of explosive phases in a star's life requires the measurement of numerous nuclear reactions involving radioactive nuclides. Most of them are studied more conveniently in the inverse kinematics mode.

In the last decade, experiments with radioactive beams have been performed in several places, including the Radioactive Ion Beam facility in Louvain-la-Neuve, where a series of beams from  $A = 6$  to  $A = 35$  were produced. The list of beams presently available with their energy range and intensity is accessible at <http://www.cyc.ucl.ac.be>.

In the course of this decade, experimental methods were developed to cope with the peculiarities of radioactive beams.

This paper deals with two different topics: i) nuclear reactions of astrophysical interest and ii) elastic scattering of radioactive nuclides. For each, methods and results will be described. The present paper does not aim at furnishing neither a complete description of the results obtained in these two fields nor a discussion of the astrophysical consequences which were deduced. Instead, the goal here is to discuss experimental topics that were not considered in previous publications, and their impact on the quality of the data.

## 2 Reaction of astrophysical interest

In hydrodynamic hydrogen burning occurring in explosive stellar situations [1], the reactions of interest are mostly of the (p,  $\gamma$ ) and (p,  $\alpha$ ) types, the former bringing the material

away from the stability line, the latter bringing it back to stability. Escape from a given cycle (in this case the hot CNO cycle) can be triggered by a (p,  $\gamma$ ) reaction (*e.g.* the  $^{19}\text{Ne}(p, \gamma)^{20}\text{Na}$  reaction), or by reactions induced on helium *i.e.* ( $\alpha, \gamma$ ) or ( $\alpha, p$ ) reactions like  $^{15}\text{O}(\alpha, \gamma)$  and  $^{18}\text{Ne}(\alpha, p)$ . This work will concentrate on (p,  $\alpha$ ) and (p,  $\gamma$ ) reactions induced by radioactive beams.

### 2.1 (p, $\alpha$ ) reactions

In (p,  $\alpha$ ) reactions in inverse kinematics,  $\alpha$ -particles are emitted in  $4\pi$  steradians. Large surface detectors are thus required. In addition, detectors should have a good angular resolution, as the angular distribution of the  $\alpha$ -particles has to be measured in order to deduce (or to confirm) the orbital angular momentum associated to the resonant states and to perform a safe extrapolation of the  $\alpha$  counts to that part of the solid angle which is not covered by the detectors.

A detector of the LEDA or LAMP type [2] is very well adapted to this problem. LEDA was in fact used several times to perform measurements of the  $^{18}\text{F}(p, \alpha)^{15}\text{O}$  reaction in different energy domains [3–5]. In all cases, the detector covered the angular region between  $12^\circ$  and  $26^\circ$  polar angle in the laboratory, with a  $1^\circ$  angular resolution. This region represented about 10% of the total solid angle. The reason for this relatively small percentage was the fact that the time-of-flight information had to be measured in order to identify particles flying from the target to the detector. A distance of 20–25 cm was found adequate to separate different species in a two-dimensional ( $t, E$ ) spectrum. The  $^{18}\text{F}(p, \alpha)$  reaction being induced by a  $^{18}\text{F}$  beam of 14 MeV on a  $\text{CH}_2$  target, the outgoing protons,  $\alpha$ -particles and  $^{18}\text{F}$  ions have typical energies of 2 MeV, 9 MeV and 6 MeV, respectively. The quality of

---

<sup>a</sup> Present address: Federal Services for Scientific Affairs, Brussels, Belgium.

the particle identification is dependent (first) on the energy resolution of the LEDA individual elements, which is typically 23 keV for 5.486 MeV  $\alpha$ -particles, including the electronic noise [2]. The second factor affecting the identification is the timing resolution governed by three factors:

- i) The time resolution of the incident beam: from a cyclotron, the beam can be given a superior time resolution only by a limitation of the phase acceptance. This is usually achieved by a slit placed near the center of the machine and resolutions of less than 1 ns [6] can be obtained that way for light-ion beams. However, this method is not applicable to our radioactive heavy-ion beams, for two reasons: 1) no further loss of intensity is tolerable, starting from  $10^5$ – $10^9$  s $^{-1}$  full beams and 2) the central region of our cyclotron has to be left free, in the acceleration in the sixth-harmonic mode. Any blocking of the beam by slits could jeopardize the separation between the radioactive beam and its stable isobar, as the cyclotron is used as a mass separator.
- ii) The phase of the beam with respect to the RF: the signals used for tagging the beam burst are in fact taken from the RF amplifiers. Any phase shift of the beam with respect to the RF will broaden the resolution of the time measurement. As such a phase shift is however a slow process, the broadening can be minimized by dividing the acquisition time in short runs, that can be corrected for a shift before summing them up.
- iii) The quality of the electronic modules (discriminators, TDCs) following the timing output of the preamplifier.

All together, time resolution of our measurements spanned the 1.5 to 3 ns range, most of which being due to the intrinsic resolution of the beam. No specific attempt was undertaken to improve this figure.

Figure 1 shows a typical two-dimensional spectrum reconstructed for a particular strip of LEDA in the measurement of the  $^{18}\text{F}(p, \alpha)^{15}\text{O}$  reaction. The RF signals, which are used to stop the TDC, are taken every second cycle only, using a rate divider. This provides with a duplication of the spectrum covering normally one RF period and it avoids the loss of that part of the spectrum in which start and stop signals are too close to each other to be registered by the TDC.

In fig. 1,  $\alpha$ -particles from the  $^{18}\text{F}(p, \alpha)$  reaction are clearly separated. A region containing the associated  $^{15}\text{O}$  ions can also be located in the  $(t, E)$  plane. Detecting the  $^{15}\text{O}$  ions appears as an attractive alternative solution as regard to the covered solid angle (much larger than for  $\alpha$ -particles). However, multiple scattering in the target makes the angular resolution much worse for  $^{15}\text{O}$  ions and in addition the loss of  $^{15}\text{O}$  counts through the central hole of LEDA ( $\varnothing$  10 cm) is not easily estimated for the same reason.

The classical particle identification by the energy loss method could be an interesting alternative to the time measurement, the former providing with a much larger solid angle (in principle). However, some practical problems are present: either one would have to add large surface  $\Delta E$  gas counters in front of the  $E$  silicon detector, or

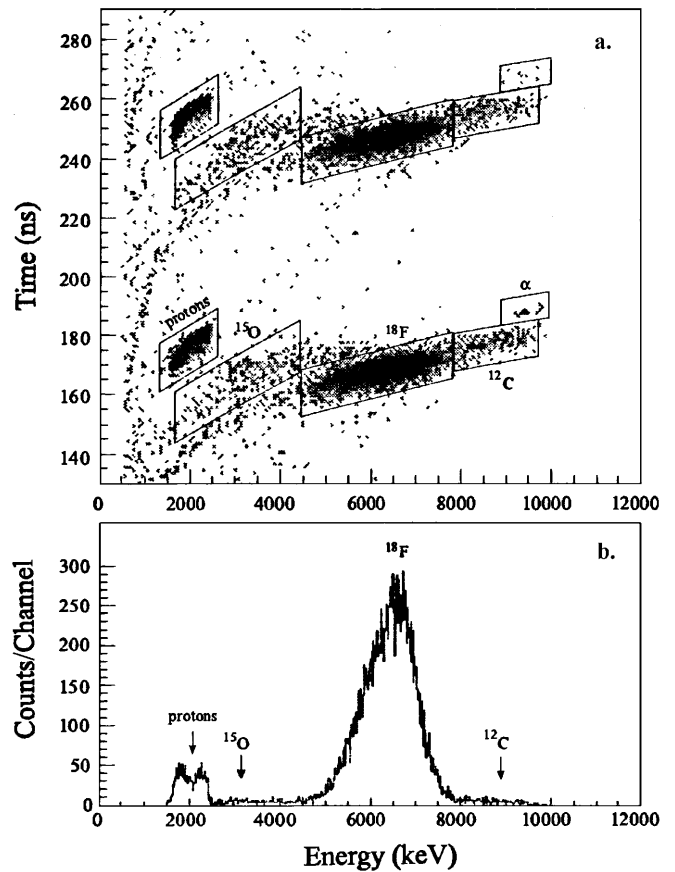


Fig. 1. a. Typical two-dimensional spectrum obtained for a particular strip of LEDA in the  $^{18}\text{F} + \text{CH}_2$  interaction. The  $x$ -axis is the energy (in keV), the  $y$ -axis is the time of flight (in ns). b. Projection of the two-dimensional spectrum on the energy axis.

“monolithic”  $\Delta E$ - $E$  silicon detectors should be used. The latter exist indeed, but not with such a large surface.

The  $^{18}\text{F}(p, \alpha)$  reaction was performed between 270 and 730 keV above threshold in the c.m. [3–5]. This domain was covered in two steps. In each, the  $^{18}\text{F}$  beam was scanning a broad range of energies while it crossed a thick  $\text{CH}_2$  polyethylene foil ( $\geq 250$   $\mu\text{g}/\text{cm}^2$ ). In the low-energy measurement (270–530 keV), the number of  $\alpha$ -particles detected was so low (a total of 47 events in LEDA) that it was impossible to reconstruct an angular distribution. Only a global spectrum was reconstructed in the c.m. In such circumstances, the background counts are an important factor to take into account, whether they originate from “internal” sources, *i.e.* activated material in the detector surroundings (*e.g.*, the Al plate supporting the detector) or from “external” sources (cosmic rays). The background was measured with no beam on target, implying that no time signature was available. In the 6–9 MeV domain, the number of events recorded was  $1.6 \pm 0.2/\text{h}/\text{cm}^2$ . The measured background events were scaled down by the ratio of the time window for  $\alpha$ -particles in the actual measurement to the RF period. To reach energies lower than 270 keV in the c.m. does

not appear to be feasible with the present  $^{18}\text{F}$  beam intensity ( $\leq 10^6 \text{ s}^{-1}$ ), unless a very strong resonance were present below 270 keV, which is not predicted by calculations [7]. In addition, measurements below 270 keV would be subject to a much larger background, as  $\alpha$ -particles from  $^{18}\text{F}(\text{p}, \alpha)$  would have then energies below 6 MeV. In the 4–6 MeV region, the background in the detector was larger by a factor of about 6 than the background in the 6–9 MeV region. This indicates that the background origin is probably actinides. Let us remark that the background could be totally suppressed by requesting a coincidence between the  $\alpha$ -particle and the  $^{15}\text{O}$  ion. Limitations quoted above about the non-obvious detection of these ions should be kept in mind. In the low-energy measurement, only one compound level in  $^{19}\text{Ne}$  was clearly excited, at 6.74 MeV, ( $J^\pi = 3/2^-$ ) for which a resonance strength  $\omega\gamma = 3.5 \pm 1.6 \text{ eV}$  was calculated. In the high-energy measurement covering the 490–730 keV energy range,  $\alpha$ -spectra were dominated by a peak corresponding to the excitation of the 7.07 MeV in  $^{19}\text{Ne}$  ( $J^\pi = 3/2^+$ ). A resonance strength of  $4.6 \pm 0.2 \text{ keV}$  was deduced for this level. Our data have allowed to calculate the stellar reaction rate for this reaction and, therefrom, the lifetime of  $^{18}\text{F}$  in the presence of hydrogen in different stellar environments. The latter quantity is relevant in  $\gamma$ -ray astronomy. The future INTEGRAL mission of ESA [8] would be able to observe 511 keV  $\gamma$ -rays from  $^{18}\text{F}$  decays following hydrodynamic H-burning in a nova phenomenon, if  $^{18}\text{F}$   $\beta$ -decay is faster than the  $^{18}\text{F}(\text{p}, \alpha)$ . ( $^{18}\text{F}(\text{p}, \gamma)$  is much slower [9]). Our data indicate that  $^{18}\text{F}$  would always react with protons before decaying. This however is true only if  $^{18}\text{F}$  remains in a dense environment after formation, which means that astrophysical models should give the answer [10].

## 2.2 (p, $\gamma$ ) reactions

This type of reactions offer the experimentalist a broad choice of detection set-up, that can fall in three categories: i) the detection of prompt  $\gamma$ -rays; ii) the direct detection of the final heavy-ion products; iii) the indirect detection of the final products through their radioactive decays, *i.e.* positrons,  $\alpha$ -particles or protons.

Each method has strong and weak points, which were detailed before by one of the authors [11]. In brief, the following considerations can be made. The first method is tractable only in a very limited number of cases, *i.e.* when the spectroscopy of the compound nucleus is well known and not too complicated. Germanium detectors can then be used to detect  $\gamma$ -rays. An example is the  $^{13}\text{N}(\text{p}, \gamma)^{14}\text{O}$  reaction. The second method is universal, *i.e.* final nuclei coming out from the target in a very narrow cone, of typically  $1^\circ$  half-opening. Beam ions are contained in the same cone, both species, having very close momenta (the  $\gamma$ -ray carries out a very small momentum), can be separated according to their different velocities. The third method can be performed in several cases, when the positron energy ( $E_\beta$ ) of the final nuclei is much larger than the one of the beam nuclei (an example is the  $^{11}\text{C}(\text{p}, \gamma)^{12}\text{N}$  reaction where the  $E_\beta$ 's are 16.4 MeV and 1.0 MeV, re-

spectively), or when the final nuclei emit protons or  $\alpha$ -particles subsequently to the positron emission (an example is the  $^{19}\text{Ne}(\text{p}, \gamma)^{20}\text{Na}$  reaction, in which  $^{20}\text{Na}$  emits an  $\alpha$ -particle in 20% of the decays). The first and third methods were performed in Louvain-la-Neuve to measure the  $^{13}\text{N}(\text{p}, \gamma)^{14}\text{O}$  [12] and the  $^{19}\text{Ne}(\text{p}, \gamma)^{20}\text{Na}$  reaction [13], respectively. A recoil mass separator (second method) is presently developed [14].

The three methods differ strongly by their respective detection efficiency ( $\epsilon$ ), defined as the ratio of the detected to the produced events.  $\epsilon$  is less than 1% in method i), about 30% in method ii) and about 1–2% in method iii). These numbers are specific for the set-up effectively used in refs. [12], [14] and [13], respectively. One should remark however that the increase in efficiency is directly related to the complexity of the set-up.

## 3 Elastic scattering

The (p, p) elastic scattering is not of astrophysical interest at first sight. Nevertheless it appeared that both the (p,  $\gamma$ ) and (p,  $\alpha$ ) reactions of astrophysical interest would benefit from the simultaneous detection of recoil protons from the  $\text{CH}_2$  target.

The first reason to measure the elastic scattering is the normalization of the (p,  $\gamma$ ) or (p,  $\alpha$ ) reaction.

Three methods appear feasible to normalize a reaction:

- i) Beam ions can be integrated in a Faraday cup. This method relies on the knowledge of the distribution of the charge states beyond the target.
- ii) Beam ions scattered from carbon nuclei in the target can be detected at forward angles in the laboratory. At low c.m. energies relevant in nuclear astrophysics, the cross-section on C is purely Coulomb. The beam intensity can be deduced, provided the scattered beam ions can be separated from carbon ion recoiling from the target at the same laboratory angle.
- iii) Protons recoiling from the  $\text{CH}_2$  target can be detected at forward laboratory angles. Proton spectra can be easily normalized to a theoretical function (see below) providing with the absolute cross-section. In fact recoil protons allow to deduce the product of the beam intensity and the proton content in the target. The ratio of scattered beam ions (ii) to recoil protons is a measure of the stability of the  $\text{CH}_2$  target stoichiometry during data acquisition.

In addition to this “experimental” reason, it appeared very soon [15] that recoil protons, because of their negligible energy loss in the target, were very sensitive to the presence of resonant states in the energy spectrum of the compound nucleus made of a beam nuclide and a proton. If such a resonant state is scanned by the beam ions while crossing the target, spectacular changes occur in the recoil proton spectra detected at forward angles in the laboratory. The proton spectra contain information on the resonance energy, orbital angular momentum, total width ( $\Gamma_t$ ) and proton partial width ( $\Gamma_p$ ), all these quantities being parameters in a global fit of the proton spectra over

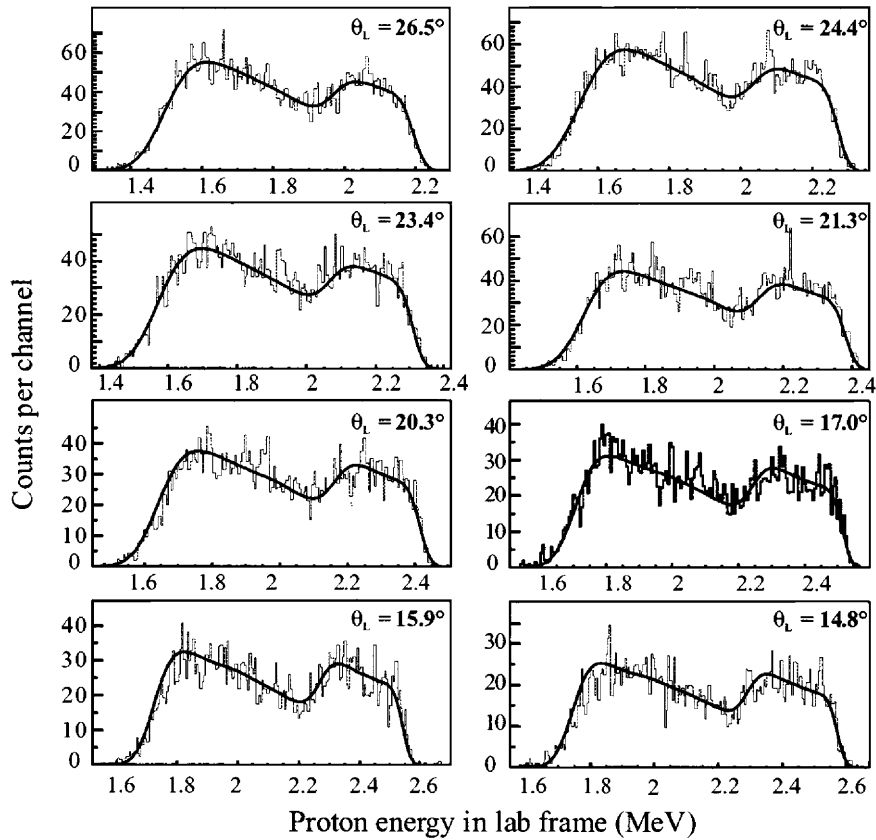


**Fig. 2.** Proton spectra from the  $^{18}\text{F}(p, p)$  elastic scattering measured at several angles in LEDA. The solid curve is the global fit to the data [5].

the angular domain covered by the detector. The fitted cross-section is the square of an amplitude containing a Coulomb and a resonant (Breit-Wigner) terms. A nice example of such a measurement is the recent work on the  $^{18}\text{F}(p, p)$  scattering [5]. Figure 1 shows a well-defined proton region in the  $(t, E)$  spectra. Figure 2 shows the projection of this region onto the energy axis at selected angles. Proton spectra were obtained at 16 angles. A global fit was performed as described above and all properties of the resonant state were deduced. This state being characterized by  $\ell = 0$ , the ambiguity between  $J^\pi = 1/2^+$  and  $3/2^+$  was removed by the following consideration: a strong correlation exists between  $J$ , the spin of the resonance and  $\Gamma_p$ , the proton partial width, in the sense that fits are sensitive only to the product  $(2J+1)\Gamma_p$ . This correlation was disentangled using a previous measurement of  $\Gamma_p/\Gamma_t$  obtained from the  $^{19}\text{F}(^3\text{He}, t)$  reaction [7]. More details on the data analysis are contained in [5].

It should be stressed that quantitative conclusions regarding the resonance parameters can be drawn only if all experimental effects are properly taken into account. Some of them are considered hereafter.

i) The energy resolution and the angular resolution of the detectors have to be incorporated, *i.e.* the theoretical expressions used to fit the data have to be convoluted with these factors. Let us remind that the proton en-

ergy in the laboratory  $E_\ell$  is given by

$$E_\ell = E_{c.m.} \frac{4A}{A+1} \cos^2 \theta_\ell, \quad (1)$$

where  $E_{c.m.}$  is the energy in the c.m. system (nearly equal to the laboratory energy in direct kinematics),  $A$  is the mass number of the beam, and  $\cos \theta_\ell$  is the laboratory angle. The factor 4 in this equation is in fact the reason why this method is working, as it gives the outgoing proton a much larger energy than in the direct kinematics mode.

The angular resolution  $\Delta\theta$  introduces an uncertainty in the laboratory energy  $\Delta E_\ell$  which, from (1), is given by

$$\Delta E_\ell = 2E_\ell \tan \theta \Delta \theta. \quad (2)$$

This results in an energy resolution varying with the angle, and modifies the shape of the interference pattern in an important way: in fact this experimental effects was mimicking an additional angular momentum component in the fit (*e.g.*, a substantial  $\ell = 2$  component in addition to the normal  $\ell = 0$ ). Taking properly into account the resolution effects in the analysis of our  $^{19}\text{Ne}(p, p)$  data totally suppressed this fictitious  $\ell = 2$  component that was originally present [16].

ii) The energy calibration of the proton spectra is an important point. In order to deduce resonance energies

from the measurement, an absolute energy calibration is indeed requested. The classical calibration using  $\alpha$ -sources has to be corrected by a factor equal to the ratio of the energy needed to create an electron-hole pair in silicon from a proton or an  $\alpha$ -particle [17]. However, proton spectra measured with a radioactive beam can also be calibrated using data obtained with the isobaric stable beam: a well-known resonance in  $^{13}\text{C}(p, p)$  scattering was used to calibrate proton spectra from the  $^{13}\text{N}(p, p)$  scattering [12]. This procedure is made very easy by the fact that in a cyclotron, a fast change between two isobaric beams is possible (it takes a minute or less).

Finally, we should mention that not all resonant states can be studied with this method, only states having a total width between 1 keV and about 50 keV being accessible. At the low boundary, the distortion to the Coulomb pattern caused by the presence of the resonance is too small to be detected, taking into account the detector energy resolution and angular resolution. At the upper limit, a resonance would require a very thick target ( $> 300 \mu\text{g}/\text{cm}^2$ ) to be covered in one step; beam straggling in the target and proton energy loss become then difficult to cope with. However, even a very narrow state could be measured if it had even a small inelastic proton width, leading to the emission of low-energy protons, below the Coulomb pattern.

This work presents results obtained in the framework of an Interuniversity Attraction Pole, financed by the Belgian State Offices of the Prime Minister, Federal Services for Scientific, Technical and Cultural Affairs. One of us (PL) is a Research Director of the National Fund for Scientific Research, Brussels. The data obtained with radioactive beams that are quoted in this paper were measured by a large collaboration from several universities, *i.e.* Brussels, Catania, Edinburgh,

Leuven, Louvain-la-Neuve, Notre Dame. We wish to thank these colleagues for their contribution. The staff of the Cyclotron Research Center in Louvain-la-Neuve is gratefully acknowledged for their dedicated involvement in the radioactive beams production.

## References

1. M. Arnould, K. Takahashi, Rep. Progr. Phys. **62**, 395 (1999); M. Wiescher, J. Goerres, H. Schatz, J. Phys. G.: Nucl. Part. Phys. **25**, R133 (1999).
2. T. Davinson *et al.*, Nucl. Instrum. Methods Phys. Res. A **454**, 350 (2000).
3. R. Coszach *et al.*, Phys. Lett. B **353**, 184 (1995).
4. J.-S. Graulich *et al.*, Nucl. Phys. A **626**, 751 (1997).
5. J.-S. Graulich *et al.*, Phys. Rev. C **63**, 011302(R) (2000).
6. S. Benck *et al.*, Eur. Phys. J. A **3**, 149 (1998).
7. S. Utku *et al.*, Phys. Rev. C **57**, 2731 (1998).
8. G. Vedrenne *et al.*, Astrophys. Lett. Commun. **39**, 325 (1999); C. Winkler, Astrophys. Lett. Commun. **39**, 309 (1999).
9. K.E. Rehm *et al.*, Phys. Rev. C **55**, R566 (1997).
10. A. Coc *et al.*, Astron. Astrophys. **357**, 561 (2000).
11. P. Leleux, in *Nuclear Astrophysics, International Workshop on Gross Properties of Nuclei and Nuclear Excitations, Hirschegg '98*, edited by M. Buballa *et al.* (GSI, 1998) p. 356.
12. P. Decroock *et al.*, Phys. Rev. Lett. **67**, 808 (1991).
13. R.D. Page *et al.*, Phys. Rev. Lett. **73**, 3066 (1994); C. Michotte *et al.*, Phys. Lett. B **381**, 402 (1996).
14. J.-S. Graulich *et al.*, *Nuclei in the Cosmos V*, edited by N. Prantzos, S. Harissopoulos (Editions Frontières, 1998) p. 471.
15. Th. Delbar *et al.*, Nucl. Phys. A **542**, 263 (1992).
16. R. Coszach *et al.*, Phys. Rev. C **50**, 1695 (1994).
17. W.N. Lennard *et al.*, Nucl. Instrum. Methods A **248**, 454 (1986).